2.1 Introduction

This chapter consisted of the material synthesis process, PBTTT-C14 and its nanocomposite film preparation via the floating film transfer method (FTM). Further, the formed FTM thin film is characterized and used for the fabrication and characterization of OTFT. To form thin films of organic semiconducting materials with optimal thickness, numerous thin film processing approaches are known such as the Spin Coating technique, Langmuir Blodgett/Langmuir Schaefer technique, floating film transfer (FTM) technique, etc. The FTM process has been presented here for the study of conducting polymer thin films for OTFTs, which is focused on its potential to fabricate devices at a cost that is significantly lower than that of traditional devices. SEM, HR-TEM, SAED, XRD, AFM, UV-Vis and CV techniques are used to analyse thin films formed using this process to estimate film quality and electronic properties. AFM, SEM, TEM, HR-TEM, and SAED pattern (acquired over Cu grid) images were obtained for morphological examination. The UV-visible spectrophotometer is used to measure the optical characteristics of the materials, FTIR to analyse functional groups' presence, and Raman spectroscopy for the identification of the vibrational modes of molecules. The thickness, phase, and shape of the films were analysed using the AFM technique in tapping mode. Kelvin probe force microscopy(KPFM) is used to measure the surface potential contrast of the film. Powder XRD is used to obtain the structural characterisation of the synthesized material using Cu-Kα radiation (λ = 1.54056 Å). Modern thin-film X-ray diffraction i.e. GIXRD technology was used to gain structural information. Each sample's incidence angle was $0.2°$. Cyclic voltammetry (CV) measurements were performed using three electrodes i.e. Ag/AgCl reference electrode, a platinum counter electrode and polymer-coated ITO working electrode cell configurations. CV was done with 0.1 M TBAP in acetonitrile at a 50 mV/s scanning rate using an electrochemical workstation (Autolab, Metrohm, USA). Desmostachya bipinnata, called Kusha in India, is used to make 2D-activated carbon. Pore size distribution and surface area were assessed using a BET analyzer. The activated carbon is used to modify the glassy carbon electrode (GCE) and was used to detect Roxarsone.

2.2 Experimental and Characterisation

2.2.1 Materials

Graphite flakes, potassium permanganate ($KMnO_4$), hydrogen peroxide(H_2O_2), orthophosphoric acid (H_3PO_4), sulphuric acid(H_2SO_4), 30% (w/v) hydrogen peroxide (H_2O_2), potassium hydroxide (KOH), hydrochloric acid(HCl), chloroform($CHCl_3$) was all purchased from Merck, India,provided the poly[2,5-bis(3-tetradecylthiophen-2-yl)thieno[3,2-b]thiophene](PBTTT-C14). Kusha grass was harvested on the campus of Banaras Hindu University. Human blood serum was taken from the institute's blood donor volunteers (courtesy: Institute of Medical Sciences, BHU, Varanasi). All experiments utilized Milli-Q water (resistivity=18 Ωcm^{-1} and pH=7.0).

2.2.2 Graphene oxide(GO) synthesis

The improved Hummers process using graphite powder is used to make GO nanosheets [251]. In a nutshell, the starting materials are 1 gm graphite flakes and 6 gm $KMnO_4$, with a 9:1 H_2SO_4/H_3PO_4 ratio (120mL:13.3mL). The mixture is then simmered for 12 hours at 55°C, stirring regularly. The inclusion of a 120 mL ice cube slows down the operation. The resulting solution is then allowed to sit at room temperature for 1 hour. To remove extra $KMnO_4$, 3 ml of 30% (w/v) H_2O_2 is added drop by drop. Finally, a brownish substance known as GO is created and given time to settle. The GO is repeatedly rinsed with distilled water and HCl until the water's pH hits 7.

2.2.3 Synthesis of reduced Graphene Oxide (rGO)

Reducing the graphene oxide with numerous reducing chemicals can increase its charge conduction. It is possible to create a material with thermal, electrical, and mechanical characteristics comparable to pure graphene using a variety of reduction methods like thermal, chemical and electrochemical. Exfoliated graphene oxide may be reduced using a variety of chemicals, including hydrazine, naphthalene, lysine, and others [252]. A high-temperature furnace generates CO_2 instead of a chemical reductant, creating enormous pressure inside the stacked layers that outweighs the Vanderwall force holding them together [253,254].

A material that is rapidly thermally expanded is the consequence of the fast evolution of gas and the subsequent thermal decomposition of GO working together in concert. Utilizing the previously acquired graphene oxide, rGO was synthesized (GO). In a quartz tube, the graphene oxide powder was heated to 400°C for an hour at a rate of 5°C/min. The end outcome was a blackish-coloured product.

2.2.4 Synthesis of Graphene quantum dots (GQDs)

In a mixed acid solution, 300 mg graphite powder was disseminated containing concentrated HNO_3(20 mL) and concentrated H_2SO_4(60 mL). The solution was then transferred to a 100 mL round-bottomed flask and agitated for 10 hours at 100 °C Following the reaction, the solution was diluted in 300 mL of deionized water before being neutralised with Na_2CO_3. Aggregation in the solution was subsequently eliminated using a 220 nm filter membrane. Finally, the material was purified using a 3500 dialysis bag [255].

2.2.5 Preparation of Graphene oxide/PBTTT-C14, reduced Graphene oxide /PBTTT-C14 and Graphene quantum dots /PBTTT-C14 nanocomposite and film formation by floating film transfer method(FTM)

The graphene oxide(GO) phase transition from water to chloroform is depicted in Fig.2.1. In conclusion, using strong sonication, uniform dispersion of 1 mg/ml of GO in an aqueous solution was produced in distilled water. A clear bi-phase was produced by adding an equivalent quantity of $CHCl_3$ to the aqueous dispersion, which is incompatible with water. The bottom layer contains $CHCl_3$, whereas the upper layer contains aqueous dispersion. The GO was transferred to the chloroform by sonicating the bi-phase solution for an hour. Following that, 200 µl of the GO/$CHCl_3$ dispersion was removed, and a solution of 10 mg/ml PBTTT (Mw= 40K-80K) was created. To ensure that the solution was evenly dispersed, it was sonicated and heated for two hours.
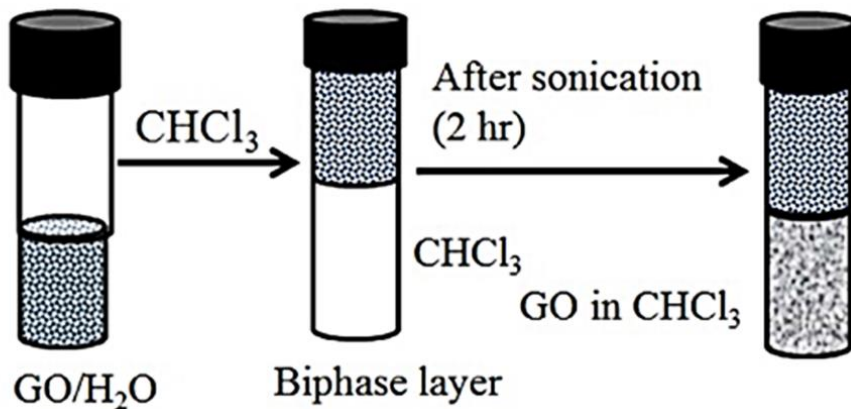
Fig.2.1 Schematic of GO transfer from the aqueous phase to the chloroform phase.

Before the PBTTT-rGO nanocomposite preparation, the 1mg/ml of rGO dispersion was prepared in chloroform by probe sonicator. Then 10µl of uniformly dispersed rGO in CHCl₃ was added to 90µl `of 10 mg/ml solution of PBTTT C-14 in a sealed tube having 1.1 % w/w filler concentration. The solution was agitated and heated for two hours at 60 °C at 30 kHz to appropriately distribute rGO in PBTTT C-14 solution. A 15 µl portion of this solution was extracted at room temperature and used to cast the film onto a hydrophilic base(ethylene glycol and glycerol in a 1:1 ratio). The as-prepared film on the hydrophilic platform was transported over a glass slide, carbon-coated grid, and silicon wafer and dried at 60 °C before various measurements and building of the OTFTs device. PBTTT/GQDs nanocomposite formation follows a similar procedure. Schematic of PBTTT/GO/rGO/GQDs nanocomposite FTM film formation is shown in Fig.2.2
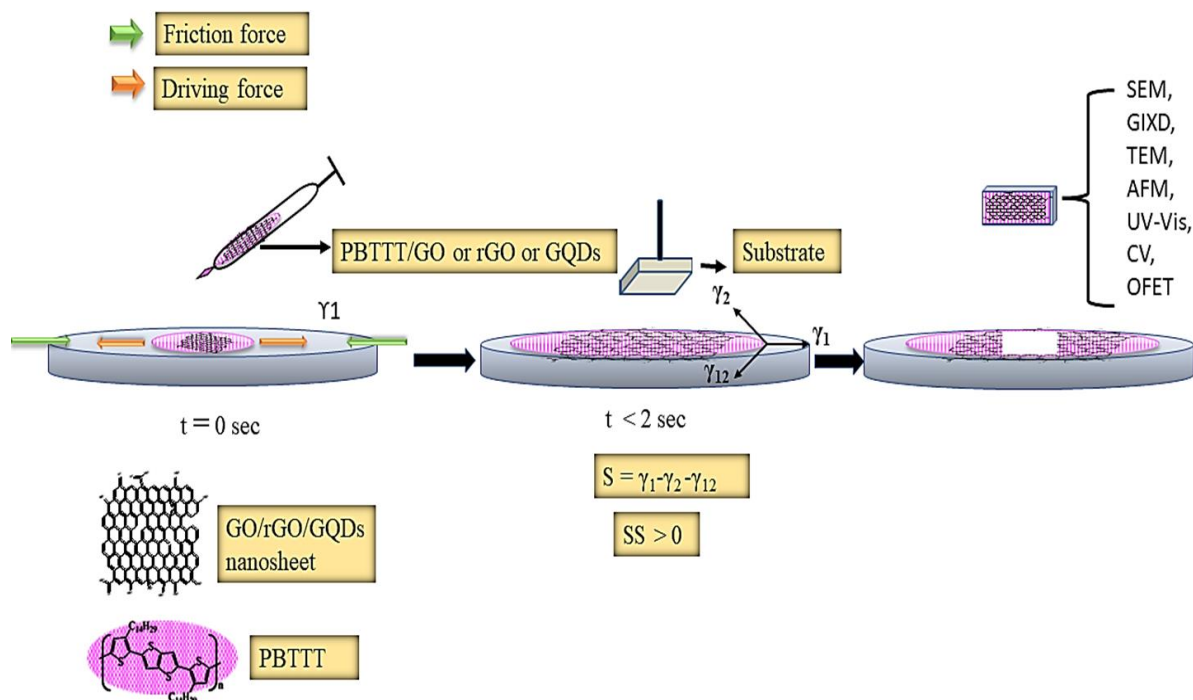
Fig.2.2 Schematic of PBTTT/GO or rGO or GQDs nanocomposite FTM film formation.

The key factor to having large-area film preparation is the solubility of polymers in various organic solvents. The solution processability of polymers improves the alignment and orientation of polymeric film and thus helps in the fabrication of thin film electronics. Various solution-based routes to deposit thin film like drop casting, spin coating, dip coating, spray coating, inkjet printing, screen printing, etc. The spin coating process is frequently utilised for thin-film device manufacturing at the lab scale for research purposes. Spray coating, inkjet printing, and slot-die coating are all common industrial applications. Each approach has its own set of benefits and drawbacks. Two other techniques viz. Langmuir Blodgett/Schaefer and floating film technique also give better uniform thin film in comparison to spin coating at lab scale.

According to the Marangoni flow, low-surface-energy solvents (such as hydrophobic dissolvable) spontaneously spread across higher-surface-energy solvents (such as

deionized ultrapure water). When a hydrophobic solvent is sprayed onto a hydrophilic surface, a surface tension differential is created at the border between the two materials. The hydrophobic solvent moves over the surface towards the parts of the surface that are more strained as a result of the surface tension difference. Meanwhile, the viscous force F_V resists the solvent's diffusion. As a result, the spontaneous spreading (SS) of hydrophobic solvent is described by the equation SS= F_D-F_V (where the driving and viscous forces are signified by F_D and F_V, respectively.).Furthermore, the spreading coefficient (S) is directly related to the equation:

$$S = \gamma_1 - \gamma_2 - \gamma_{12}$$

where γ_1 signifies the surface tension of a 1:1 mixture of ethylene glycol and glycerol acting outward, γ_2 denotes the surface tension of polymer dispersed chloroform acting inward, and γ_{12} represents the interfacial surface tension of two liquids acting inward when dropping. in Fig.2.16. The spreading process will occur naturally if the spreading coefficient is positive. The polymer self-assembly occurs simultaneously with the evaporation of the volatile solvent, resulting in an evenly compacted excellent film. $CHCl_3$, ethylene glycol, and glycerol have surface tensions of 27.5, 47.7, and 64 mN/m, respectively. Chloroform has a positive S value over a mixed hydrophilic liquid substrate

2.2.6 Synthesis of 2-D Activated carbon from Kusha grass(Desmostachya bipinnata)

Kusha grass was purchased locally and split into small pieces. Following that, it was cleaned with DI water several times. Kusha grass was cleaned and dried at 100 degrees Celsius in a vacuum oven. After that, carbonization was done in a muffle furnace at 700°C for 2 hours at a heating rate of 5.8°C min^{-1}. It was then crushed into a powder and chemically activated in a 1:3 ratio with KOH w/w. To make a homogeneous mixture, a mortar and pestle were utilised. This mixture was also given a shot of DI water, and the aqueous solution was stirred regularly overnight. In a tube furnace, the slurry was transported to a crucible and preserved in an inert argon atmosphere. The preparation of activated carbon is depicted schematically in Fig.2.3.
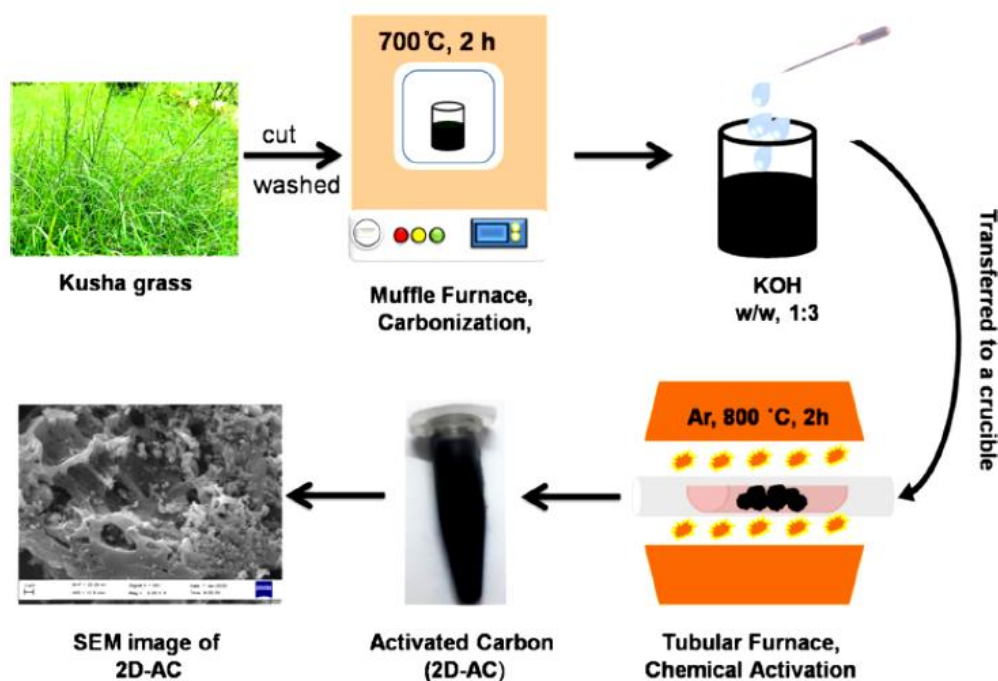

Fig.2.3 Activated carbon in two dimensions(2D) is depicted graphically.

2.2.7 OTFT Fabrication and its Characterization

2.2.7.1 Vacuum Coating Unit

The vacuum thermal evaporation unit is a device for depositing thin films of the required thickness on compatible surfaces. To evaporate the source material in the form of vapour particles, the filament must be heated at high vacuum and low pressure (around 10-6 torr). By producing the patterned thin film as required over the substrate, these vapour particles are allowed to flow freely and condensed back to their solid state form. The photograph of the vacuum coating unit (Hind HIVAC‖model No-12A4D, India) is shown in Fig.2.4. It is made up of an electric variac that regulates the flow of current to allow for regulated filament heating. During the deposition of source materials, the deposition rate, deposition angle, film thickness, and substrate temperature may all be changed. Inside the cleaned closed chamber, a vacuum is formed by the diffusion pump, which is backed up by a rotary pump. To avoid any interactions between the evaporant and the ambient air constituents, thermal evaporation activities are carried out under a high vacuum. The quartz crystal microbalance, which is based on the concept of resonant frequency change, is used to track the thin film's growth during the deposition process. The frequency shift is proportional to the amount of mass deposited on the crystal. The relative location of the evaporation source material and the targeted substrate, the cleanliness of the vacuum chamber, the substrate temperature, and the evaporation rate all affect the thin film's quality (such as uniformity and crystallinity). To deposit the desired thin film pattern, the shadow mask technique is used.

Fig. 2.4 Vacuum thermal evaporation unit (Hind HIVAC" model No-12A4D, India).

2.2.7.2 Oxidation Furnace

The oxidation furnace used in this thesis is to grow the SiO_2 layer on top of the Si substrate. The "mini-Brute" bench oxidation furnace (model no. MB71) is purchased from Thermco Inc., USA; which is shown in Fig.2.5 . The process tubes have an outside diameter of 3.25 inches and a 14-inch flat zone with a three-zone heating element that is wound constantly using a helical coil with a temperature precision of 0.5 °C. The Ana-lock (model 431) temperature controller broad sense is used to set the temperature between 200 and 1200 ° C. This furnace incorporates a water cooling system to keep the temperature in the room from becoming too high. This is only conceivable if the heating chamber's 60 % BTU (British thermal unit) is dissipated. Air cooling, in addition to water cooling, is needed via a high-volume circulating fan that runs quietly to keep all operating components safe throughout rising temperature operation.

.

Fig. 2.5 Oxidation furnace (model no. MB71, Thermco Inc., USA).

2.2.7.3 Electric oven

The sample is dried in an electric oven shortly after the thin film has grown in an inert atmosphere to maintain its properties. This oven is made out of a thermally separated chamber with a simple thermostat that allows the temperature to be regulated between 100 and 125 ° C. It also allows for fine temperature regulation and may be instantly calibrated to a pre-set temperature. The electric oven used in this thesis is obtained from Metzer Biomedical and Electronics Pvt. India Ltd. and it is shown in Fig. 2.6.

Fig. 2.6 Electric Oven

2.2.7.4 Device Characterization Setup

As shown in Fig.2.7, the device properties were analyzed using a semiconductor device analyzer (Keysight B1500A). This tool was used to evaluate the charge transfer properties of the manufactured device. To evaluate the sensor's performance, the standard source configuration of OTFTs was used. The surrounding environment was maintained at a stable temperature of 25°C and relative humidity (RH) of 54 %during the measurements.
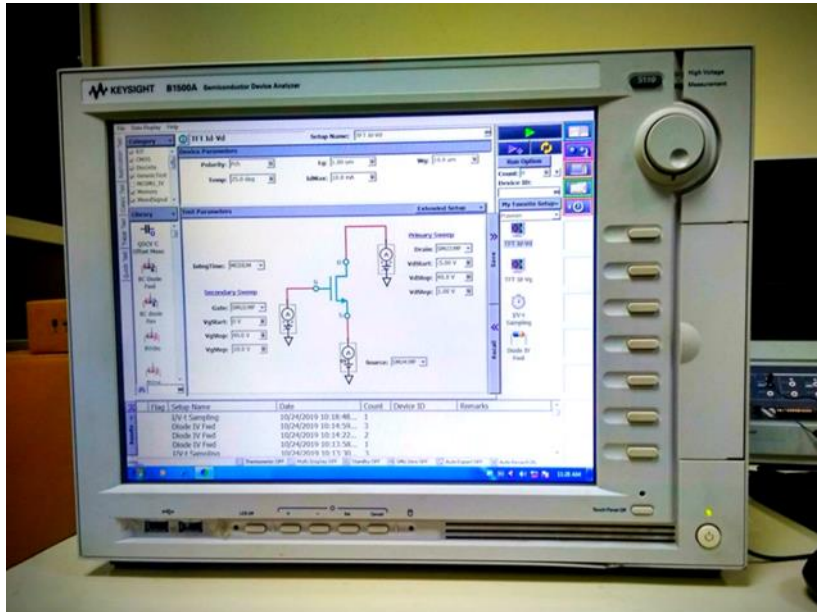
Fig. 2.7   Semiconductor parameter analyzer.

2.2.8 UV-Vis. absorptions spectrophotometry

It pertains to absorption or reflectance spectroscopy in the ultraviolet and visible wavelengths in the electromagnetic spectrum. The main idea within the molecule is that electrons are excited from a lesser electronic energy level to a higher electronic energy level. Because electrons can connect in a variety of ways, a specific amount of energy is needed to promote them. This is due to the absorption of light at various wavelengths. It specifies the type of solute present in the solvent as well as its concentration. Molecules containing bonding electrons(σ and π) and non-bonding electrons (n) are excited to antibonding σ^* and π^*. Four different sorts of transitions may be used. (π–π^*, n–π^*, σ–σ^*, and n–σ^*), and they can be ordered as follows:σ–$\sigma^* >$ n–$\sigma^* >$ π–$\pi^* >$ n–π. According to Beer-Lambert law, the light absorbance is directly related to the sample's concentration and path length for a given substance by eqn 2.2.

$$A = \varepsilon \, l \, c \qquad\qquad (2.2)$$

Where, A= absorbance

ε **= molar extinction coefficient**

l = path length of the solution

c = concentration of absorbing species

Basic instrumentation is given in Fig.2.8. The spectrophotometer Perkin Elmer Lamda-25 from Germany was used to record the electronic absorption spectra of the samples.
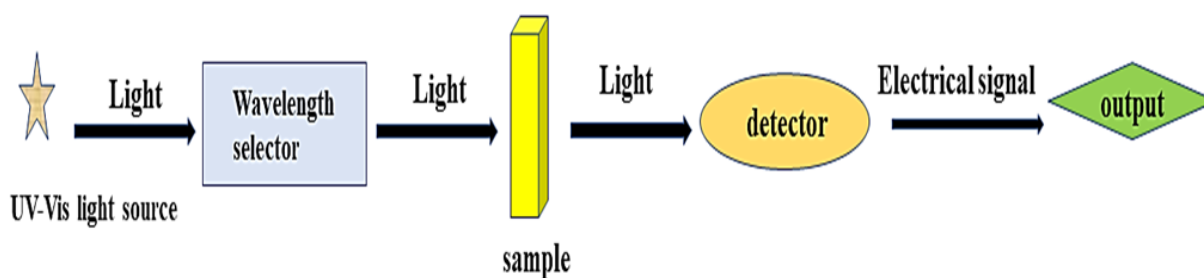

Fig.2.8 Basic instrumentation of UV-Vis spectrophotometer.

2.2.9 Fourier Transform Infrared Spectroscopy

It is put to use to get the infrared spectrum of the absorption or emission of a solid, liquid, or gas. Using a method of mathematics known as the Fourier transform, it changes unprocessed data into the actual spectrum, for example by transforming an interferogram. In this scenario, infrared light is allowed to pass through the sample, and a sample spectrum is obtained as a result of part of the radiation being absorbed while another radiation is transmitted. Specific chemical groups contained in the sample may be characterized using spectral data and the infrared absorption frequency, which ranges from 600 to 4000 cm^{-1}. FT-IR offers information on unidentified compounds and can calculate amounts in a mixture. A fingerprint of the sample is produced by the infrared

spectrum's absorption peaks, which are related to the frequency of oscillations between the bonds of the atoms in the sample. No two substances will have the same infrared spectrum since each sample is made up of an irregular mixture of atoms. Infrared spectroscopy, therefore, offers a conclusive identification (qualitative analysis) of all kinds of materials. The size of the peaks in the spectrum also shows how much substance is there. Fig.2.9 shows a schematic diagram of the FT-IR spectrometer. Thermo 5700 FT-IR spectrometer, Germany, was used to record the FT-IR spectra of all the samples.
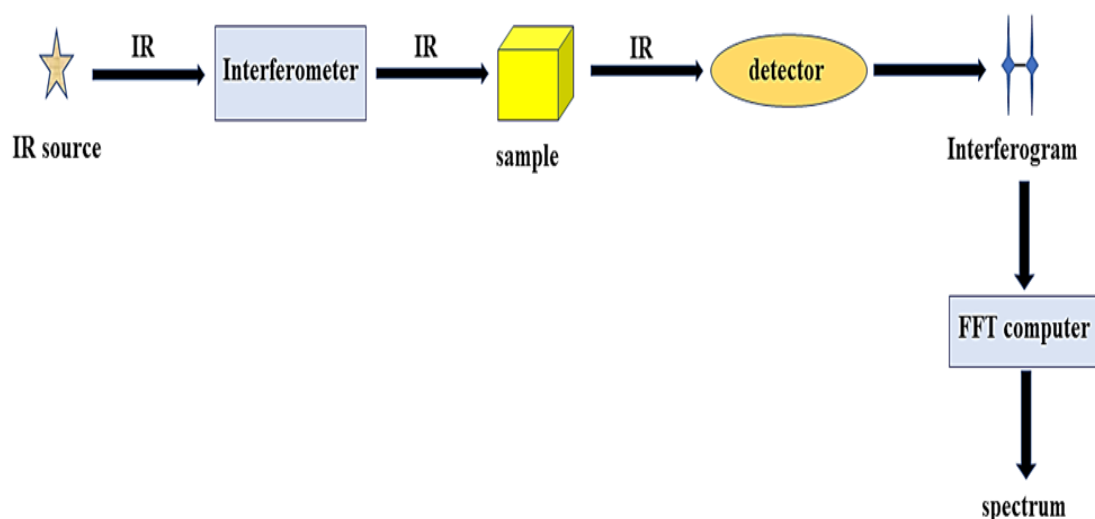
Fig.2.9 Basic instrumentation of FT-IR spectrometer

2.2.9 Raman spectroscopy

It is a non-destructive analytical technique which determines the vibrational modes of molecules. Raman spectroscopy works based on the idea that when monochromatic light passes through a sample, it may be reflected, absorbed, or scattered. The vibration and rotational properties of the scattered photons cause them to have a different frequency from the incident photon. There are two types of scattering processes: Rayleigh scatters and Raman scatter. In Rayleigh scattering, the scattered light is of the same wavelength as the laser source which does not give useful information about the

sample. While in the Raman scatter, the scattered light is of different wavelengths depending upon the molecular structure. It is also called the inelastic scattering of photons. Wavenumbers with inverse length units are commonly used to describe Raman shifts. In the Raman spectra, the wavelength and wavenumbers of shift may be converted using the formula below:

$$\Delta\tilde{\nu} = \left(\frac{1}{\lambda_0} - \frac{1}{\lambda_1} \right) , \qquad (2.3)$$

where $\Delta\tilde{\nu}$ is the Raman shift in wavenumber, λ_0 is the excitation wavelength, and λ_1 is the wavelength of the Raman spectrum. The Raman spectra were collected using an SPR 300 Raman spectrometer with a 532 nm stimulating laser source.
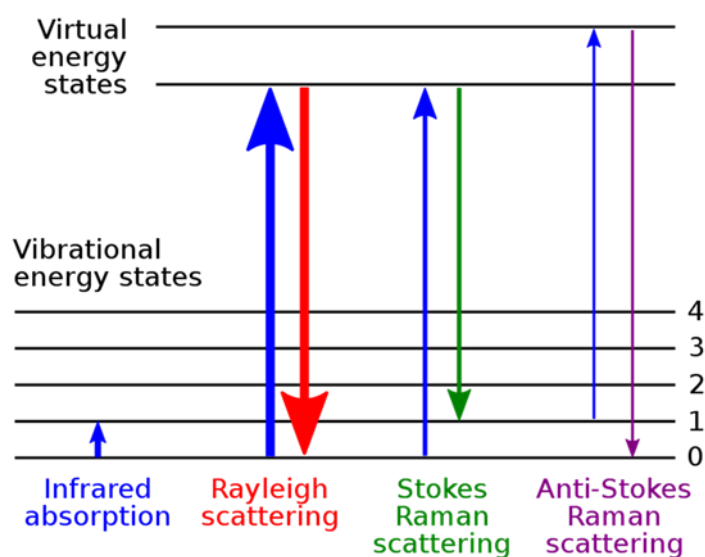

Fig. 2.10 Raman principle

2.2.10 Cyclic voltammetry

It's utilised to investigate a system's electrochemical behaviour. The application of potential (E) to an electrode and observation of the resulting current(i) is a common aspect of all voltammetric techniques. The voltammetric cell consists of three electrodes viz. working, counter and reference which are connected to the power supply as shown in Fig.2.11. Working electrodes come in a variety of shapes and materials, ranging from microscopic Hg drops to flat platinum, gold, and glassy carbon discs. Auxillary or counter electrodes enable current to flow through them, balancing the current at the working electrode. A reversible half-cell response with Nernstian behaviour is provided by the reference electrode. It serves as a reference for monitoring and adjusting the potential of the working electrode. The voltage at the working electrode is increased linearly with time in a Cyclic Voltammetry (CV) experiment. The cyclic voltammogram plot is obtained by drawing the current at the working electrode versus the applied voltage. It investigates the redox and transport mechanisms of a system in solution. In CV, the potential is linearly changed over time with two extreme values. The peaks in CV can be used to calculate the HOMO or LUMO by the following formula:

$$E_{HOMO} = -[E_{OX} - E_{1/2 \text{ (ferrocene)}} + 4.8] \text{ eV} \tag{2.4}$$

Where E_{OX} is the peak value of CV's current voltage, and $E_{1/2}$(Ferrocene) is the ferrocene's half oxidation potential[256]. Three electrode cell assemblies were used for cyclic voltammetry (CV) measurements, using Ag/AgCl as the reference electrode and polymer-coated ITO as the working electrode. CV with 50 mV scanning rate in the range of 0.0V to 1.3V versus. Ag/AgCl was carried out utilising an electrochemical workstation and 0.1M tetra butyl ammonium perchlorate (TBAP) in Acetonitrile (Autolab, Metrohm, USA). The ITO electrode was washed with distilled water, acetone and isopropyl alcohol for 10 min. each. For the electrochemical sensing Roxarsone drug, a glassy carbon electrode(GCE) (disc electrode, diameter=3mm) was used as a working electrode. It was polished with alumina slurry (particle size=0. 4µm) over a polishing pad before using GCE. After that, the surface was cleaned in an ultrasonic

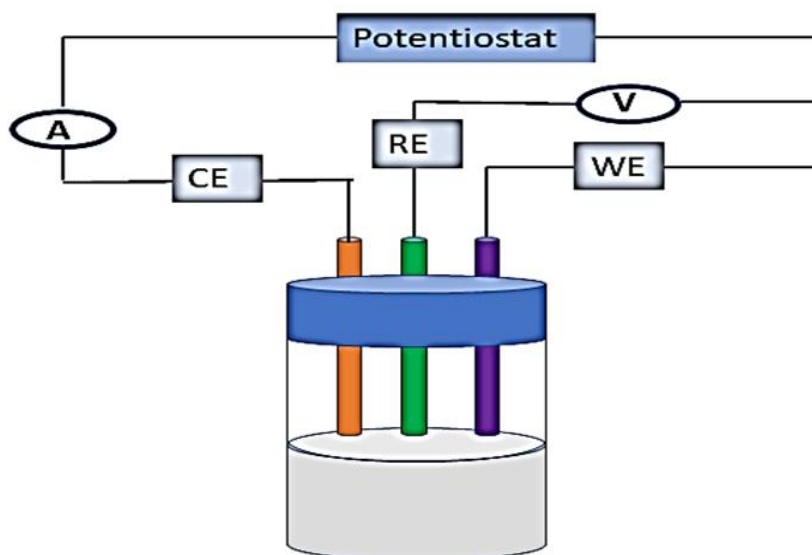bath with acetone. The sample was then cast over the electrode and allowed to dry at room temperature.

Fig.2.11 Schematic representation of experimental setup in Cyclic voltammetry.

2.2.11 Scanning electron microscopy(SEM)

It's a sort of electron microscope in which a raster pattern of high-energy electrons is swept across the surface. The interaction of electrons with atoms in the sample provides information on the sample's surface topography and composition. It consists of an electron gun, electromagnetic lenses and detectors. Backscattered electrons (BSE) and secondary electrons (SE) are the two types of electrons employed in SEM to scan the material (SE). After an elastic contact between the beam and the sample, BSE is reflected. Because of the inelastic contact between the beam and the sample, SE originates from atoms in the sample. The essential components of SEM are shown in Fig. 2.12. Carl Zeiss Supra 40 SEM pictures of samples were collected for morphological investigation (New Zealand).
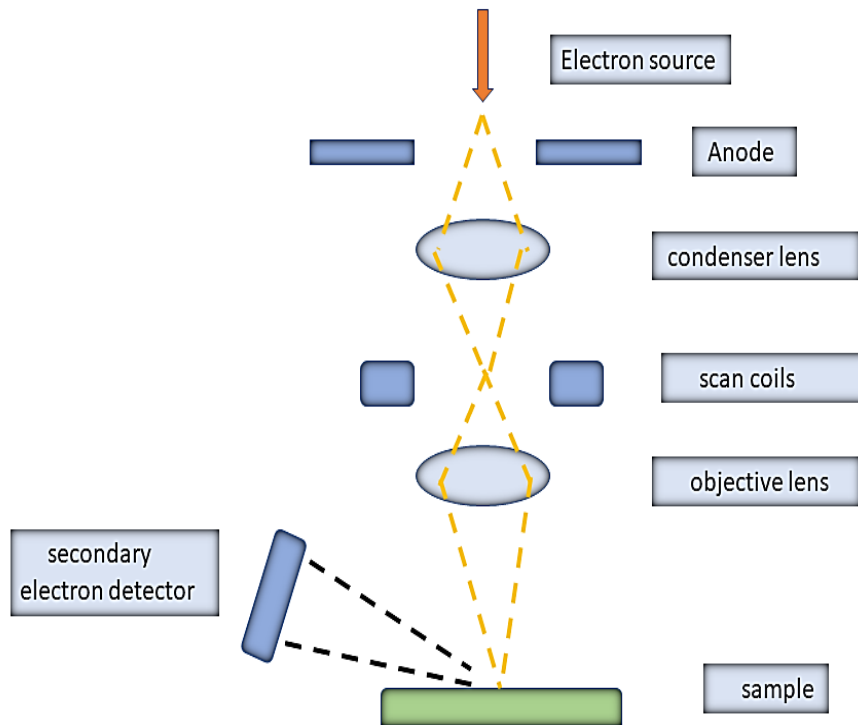
Fig.2.12 Schematic representation of basic components of SEM.

2.2.12 Transmission electron microscopy(TEM)

It's an electron microscope in which a high-energy electron beam (100-400 keV) is permitted to travel through an ultrathin material, interacting with it as it passes. The picture is amplified and focused onto an imaging device, phosphor screen, or charge-coupled device (CCD) camera following the encounter. Because electrons have a shorter de Broglie wavelength, they can photograph at a better resolution than an optical microscope. The sample is prepared specifically for TEM and put inside the vacuum chamber, which is then evacuated of air. It comprises an electron source, or cathode, constructed of tungsten filament or a single lanthanum hexaboride crystal. The cannon is attached to a high-voltage source (about 100-300 kV) that delivers enough current for it to begin releasing electrons into the vacuum. After leaving the cannon and reaching the next part of the microscope, the condenser system, the electron beam is accelerated

by electrostatic plates. These lenses focus an electron beam on a sample of a certain size and location. A resolution of ~ 0.1 nm is obtained in TEM images with ~ 500 KX magnification which is many times larger than the optical images. The morphological, crystallographic and compositional information is studied by TEM. Tecnai G2 (New Zealand) was used to get the HR-TEM and SAED pattern over the Cu grid. The essential components of TEM are shown in Fig.2.13.
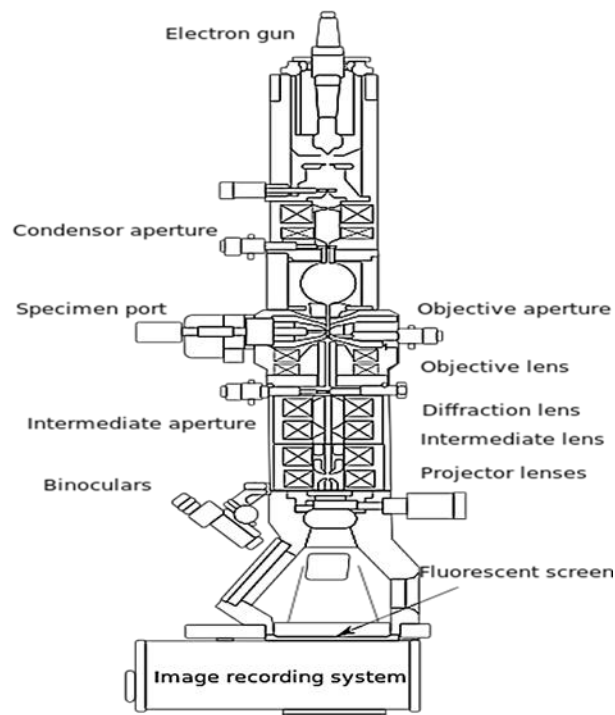

Fig.2.13 Schematic representation of basic components of TEM(Wikipedia)

2.2.13 Atomic Force Microscopy

Scanning probe microscopy (SPM) is also used to examine the morphological surface (roughness) of the polymer thin film. The physical probe is used to scan the surface profile data of the sample surface (tip). It includes information on atomic force microscopy (AFM), scanning tunnelling microscopy (STM), near-field scanning optical microscopy (NSOM), and other microscopy techniques. It operates by using an AFM

probe with a pointed APM tip to sweep a raster-like pattern throughout the sample surface. A silicon or silicon carbide tip is attached to the free end of the AFM cantilever tip. The cantilever tip used in AFM has a radius of a few to tens of nanometers. The cantilever deflects when the tip makes an encounter with a sample surface as a result of forces between the tip and the sample. In contact mode, the tip is "dragged" through the sample's surface, and the surface contours are either directly calculated from the cantilever's displacement or indirectly via the feedback controller needed to maintain the cantilever's position. Most samples generate a liquid meniscus layer under typical circumstances. Therefore, a significant challenge for contact mode in ambient settings is to maintain the probe tip near the sample to record pretty short forces while preventing it from adhering to the surface. Using a dynamic contact mode solved the issue (also known as intermittent contact, AC mode, or tapping mode). The cantilever is forced to bounce upwards or downwards at or near its resonance frequency while in tapping mode. The cantilever tip does not come into contact with the sample surface while using atomic force microscopy in the non-contact mode. Instead, the cantilever oscillates with an amplitude varying from a few nanometers (10 nm) to a few picometers at or just over its resonance frequency (frequency modulation). The AFM equipment used in this work for semiconducting material investigation was provided by NT-MDT Services and Logistics Ltd. (model NTEGRA Prima), Ireland. The tapping mode in AFM is depicted schematically in Fig.2.14.
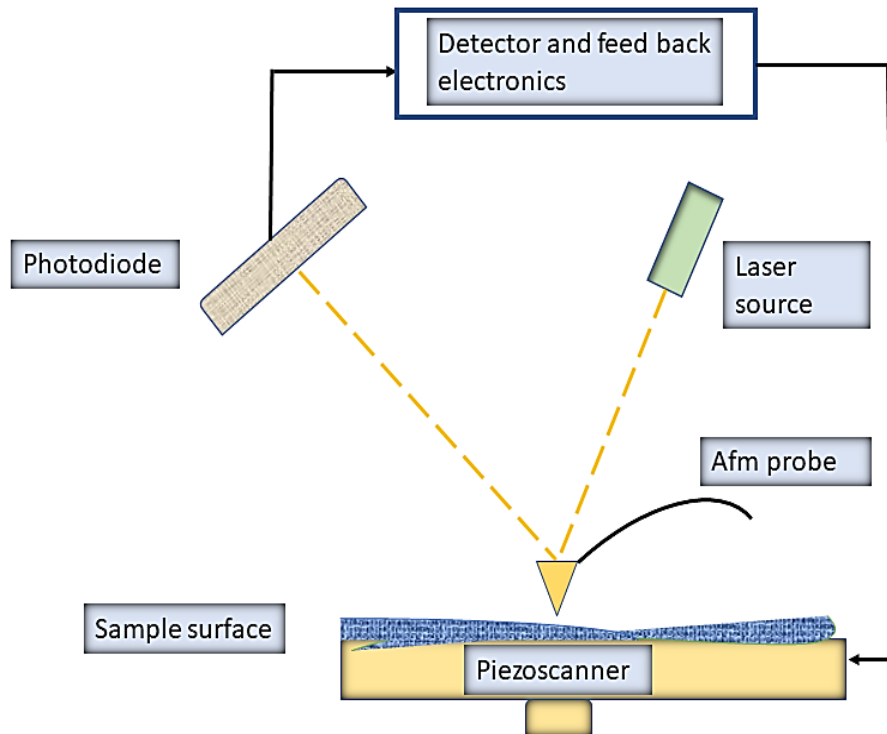
Fig.2.14 Schematic representation of tapping mode in AFM.

2.2.14 X-ray Diffraction (XRD)

X-ray diffraction (XRD) examination examines the crystallographic structure of any synthetic or natural material whose crystalline structure diffracts incoming X-rays. Crystallographers measure the angles and intensities of diffracted beams to determine the crystal's electron density. This electron density may be used to compute atom locations, chemical bonding, and crystallographic disorder. X-rays are electromagnetic energy waves, and crystals are atoms organised regularly. Atoms' electrons scatter X-rays. When an X-ray hits an electron, a secondary X-ray emerges. The electron scatters in elastic scattering. A scattering array creates spherical waves. Although destructive interference cancels these waves in most directions, Bragg's law specifies that they contribute constructively in a few directions:

$$n\,\lambda = 2d\,\sin\theta \qquad\qquad \textbf{(2.5)}$$

Where n stands for an integer, d is the interplanar distance, θ is the incidence angle, and λ is the wavelength of the radiation. These exact orientations are shown by the reflections, which are dots on the diffraction pattern. Thus X-ray diffraction occurs because of the electromagnetic wave(X-ray) striking on a repeating arrangement of atoms within the revision. The diffraction pattern is created by X-rays because their wavelength is typically on the same order of magnitude (1-100 Å) as the separation d between crystal surfaces. The XRD measurements of the thin films examined in this thesis work were performed using a Smart Lab X-Ray Diffractometer, Rigaku, Japan.
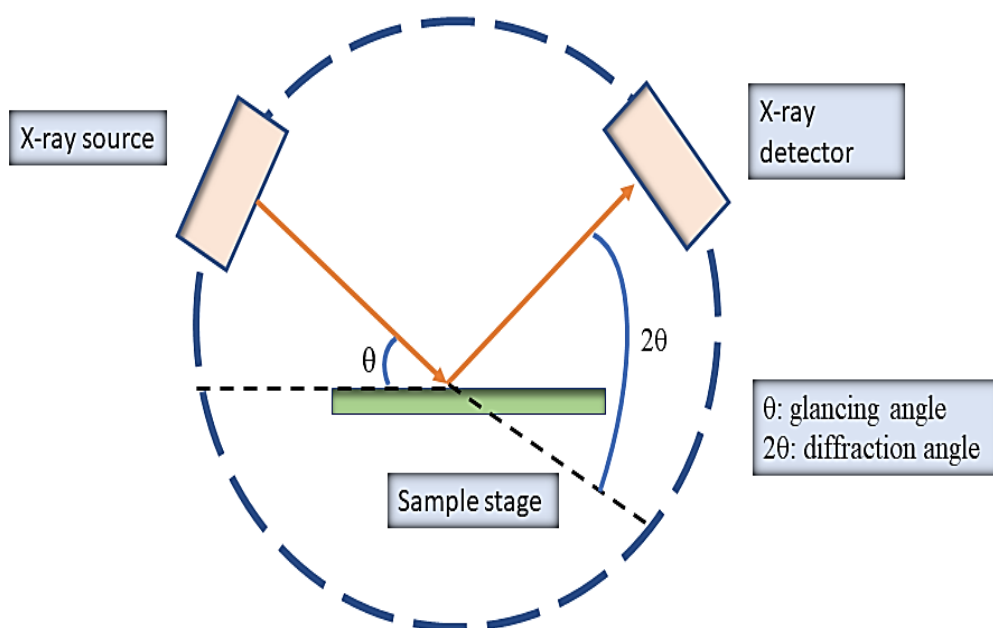
Fig.2.15 Schematic representation of X-ray diffraction.

2.2.15 BET Surface Area Analyzer

The tool is made to conduct physisorption and chemisorption investigations. The device must carry out the following tasks: it must assess the precise surface area of the materials in their various physical configurations; it must also ascertain other data including gas absorption, micropore volume, and pore size distribution. The Brunauer-Emmett-Teller (BET) theory is a key analytical tool for the assessment of the specific surface area of materials. It seeks to explain the physical adsorption of gas molecules on

a solid surface. Physical adsorption or physisorption is a term that is frequently used to describe the findings. In the Journal of the American Chemical Society, Stephen Brunauer, Paul Hugh Emmett, and Edward Teller published their idea in 1938. The BET theory applies to multilayer adsorption systems that typically employ a probing gas (referred to as the adsorbate) that does not chemically interact with the adsorptive (the substance that the gas adheres to; the gas phase is referred to as the adsorptive). The most popular gaseous adsorbate for exploring surfaces is nitrogen (s). Due to this, routine BET analysis is often carried out at N_2's boiling point (77 K). To quantify surface area at various temperatures and measurement scales, other probing adsorbates are also used, albeit less frequently. These consist of water, carbon dioxide, and argon. Quantities of the specific surface area obtained by BET theory may be affected by the adsorbate molecule used and its adsorption cross-section because the specific surface area is a scale-dependent feature with no one true value specified.

Fig.2.16 BET Surface Area Analyzer.

2.2.16. Fabrication of PBTTT C-14-based transistor.

Organic transistors are made by depositing a well-defined electrode on an organic thin layer that is supported by a SiO_2/Si substrate. The present work employed the FTM approach to developing the thin film of organic semiconductors over the self-assembled monolayer (SAM) modified insulating layer (SiO_2).

2.2.16.1 Substrate Specifications

The Si substrate is employed to fabricate the organic transistors. The low surface roughness of the developed insulating layer (SiO_2) over highly doped silicon eliminates the problem of lattice mismatch during thin film deposition, allowing the substrate to function as the gate electrode for bottom contact devices.

Substrate: Silicon (Monolithic semiconductor)

Surface: One-sided polished

Type: p-type <100>

Diameter: 75±2 mm

Thickness: 300-350 μm

Resistivity: 3-5 Ω-cm

2.2.16.2 Substrate Cleaning

The process used to clean the substrate in our laboratory's clean room is outlined below:

(i)   The impurities are introduced to the wafers throughout the slicing, polishing, lapping, and packing processes. These impurities may be readily removed from the wafers using ultrasonication for about 5 minutes before dipping them in trichloroethylene (TCE)

(ii)   The oil and organic residue on the polished surface of the wafer can be cleaned even further by soaking the wafers in Acetone for 1-2 minutes.

(iii)   After washing the wafer with Acetone, de-ionized (DI) water with a resistivity of 18 MΩ is used to rinse it 4-5 times.

(iv)   A mixture of H_2SO_4 and H_2O_2 in the ratio of 4:6 is made, and the dry wafer is submerged in it for 5 minutes. After that, the wafer is washed in DI water that is flowing.

(v)   For greater cleanliness, the wafer is washed in DI water 2-3 times more.

(vi)   Another solution of HF and DI in the ratio of 1:6 is made, and the wafer is immersed in this solution for 1 minute before being washed in DI water 10-15 times.

(vii)   Furthermore, the wafer is washed 10-15 times with DI water.

The wafer is now placed on a Petri dish and dried completely for 10 minutes in an electric oven set to 100°C.

2.2.16.3   SiO₂ growth

The dry oxidation process is carried out thermally on the substrate in the furnace. It involves a regulated flow of oxygen gas inside the furnace's Quartz tube, ensuring that enough gas is available for the silicon wafer to oxidise. A mixture of oxygen/nitrogen (3:1) is blasted into the furnace tube during the formation of the oxide layer on the silicon substrate. Following is the chemical reaction for oxidation:

$$Si + O_2 \longrightarrow SiO_2$$
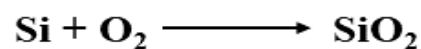
This oxidation process occurs at a higher temperature (more than 1000 °C). Before turning on the temperature controller's ON switch, water is pumped throughout the furnace for cooling. The centre zonal temperature is set using the temperature dial attached to this furnace, and nitrogen flow is then supplied within the tube to produce an inert atmosphere. During the oxidation process, a flow metre linked to the furnace is used to control the flow of nitrogen and oxygen gases. The nitrogen and oxygen gas flow rates are maintained at 0.6 and 1.8 litres per minute, respectively. When the furnace's centre zonal temperature reaches the correct level, the wafer is placed inside

and the needed gas mixture flow is maintained for the predicted time duration. Dry oxidation is the term for this process. The thicker oxide layer (> 300 nm) is generated using the wet oxidation approach, in which water vapour is combined with the nitrogen and oxygen gas flow during the oxidation process. The formation of the oxide layer is also influenced by the water vapour concentration, with larger concentrations resulting in quicker but lower-quality growth. In most OTFT designs, a thicker oxide layer is employed to shield the transistor from gate leakage current. After the oxide layer has reached the desired thickness, the flow of oxygen gas is turned off, and the furnace's heating element is turned off. The flow of nitrogen gas is, nevertheless, maintained until the furnace temperature reaches room temperature.

2.2.16.4 Growth of self-assembled monolayers (SAMs) over SiO$_2$

The use of a SAM layer improves the electrical performance of OTFT devices in this thesis. For top-contact bottom-gated devices, this layer is formed over the SiO$_2$/Si substrate. Numerous SAMs such; as octadecyl trichlorosilane (OTS), cyclized transparent optical polymer (Cytop), and hexamethyldisilazane (HMDS), etc. are employed to treat the OTFT oxides; where OTS is typically used. During the OTS treatment, the passivation of –OH groups (which sit on the oxide surface) affects the threshold voltage of an OTFT, enhancing the mobility of the charge carriers. The presence of humidity during the OTS treatment is critical for the OTS molecules to bond to the oxide surface. The increased water content, on the other hand, may cause OTS molecules to partially cling to the oxide surface. To make the oxide surface more hydrophobic, the SiO2 surface is treated with OTS by soaking it in a 10mM OTS solution (in toluene) at 60°C for 45 minutes. This procedure is carried out to make the surface of the oxide more hydrophobic. OTS-treated substrates were thoroughly cleaned with toluene before being heated at 120°C for 30 minutes before the deposition of the polymeric thin film.

2.2.16.5 Electrode deposition for source-drain (S/D) contacts

Gold (Au) and Palladium (Pd) are the source-drain contact materials utilised in OTFT construction (Pd). These electrode materials have a larger work function (> 5 eV), ensuring that p-type organic semiconductors have the optimum ionisation potential match. It also has a low potential barrier at the metal/semiconductor contact, allowing

for good charge carrier transmission. For S/D electrode metal deposition, gold is a natural candidate. The thermal evaporation of Au & Pd metal electrodes is done by using a Vacuum evaporation unit. These thermally evaporated metal electrodes are formed as wires and stored inside a tungsten boat heating element. The patterning of the deposited S/D electrodes was achieved by selecting the suitable shadow mask dimensions. This shadow mask should be positioned correctly to produce the requisite channel length and breadth of sharp S/D metal electrodes. Any misalignment in this regard may have an impact on the produced devices' electrical performance. The silver (Ag) paste is also applied to the strongly doped Si substrate, which is employed to construct an OTFT gate terminal. The solubility of this solution-processable electrode is excellent, and it oxidises very little in the environment.

2.2.16.6 Construction and Working of Organic thin-film transistor

A thin film transistor is an electrical device that uses an electric field to regulate the flow of current across a semiconductor layer. A field-effect transistor (FET) is another name for it FETs are three-terminal devices: source, drain and gate. The conductivity across the channel between the source and drain may be controlled by applying a voltage to the gate terminal. Because they may employ either electrons or holes as charge carriers, FETs are unipolar transistors. The concept of FET was first used by Julius Edgar Lilienfeld in 1930 [257]. The Si-based FET i.e. metal-oxide-semiconductor FET was first designed by Kahng and Atalla in 1960 [258]. Usually, single-crystalline Si is used to get a good Si/SiO_2 interface in MOSFET. Barbe et al. [259], Petrova et al. [260], and Ebisawa et al. in 1983[261] were the first to examine the field effect in organic semiconductors. In 1987, Koezuka and colleagues discovered organic FETs employing polythiophene as an active semiconducting material [262]. Tsumura et al. used electrochemically polymerized polythiophene as an active p-type semiconductor in 1988 [263]. OFETs are currently widely employed in low-semiconductivity materials, and their efficacy is equivalent to that of amorphous silicon FETs, allowing them to replace amorphous silicon FETs in large-area circuits.

Organic thin-film transistors (OTFTs) are three-terminal field-effect transistors (FETs) with a source, drain, and gate electrode. The charge is transferred between the source and drain terminals. The gate terminal is used to provide the electric potential to regulate charge transfer between the source and drain. As illustrated in Fig.2.16, there

are four primary OTFT designs: top-contact top-gate, top-contact bottom-gate, bottom-contact bottom-gate, and bottom-contact top-gate. The heavily doped silicon is used as a common electrode i.e. gate contacts for all the OTFT bottom contact substrates. The insulating dielectric gate oxide i.e. silicon oxide is grown on a silicon substrate by thermal oxidation. Any holes and cracks on the dielectric layer may cause leakage through the gate terminal, therefore surface treatment by a self-assembled monolayer(SAM) is necessary before depositing any active material on SiO_2 grown substrate. Next high work function metal is deposited on the polymer active layer to have source and drain contact electrodes.
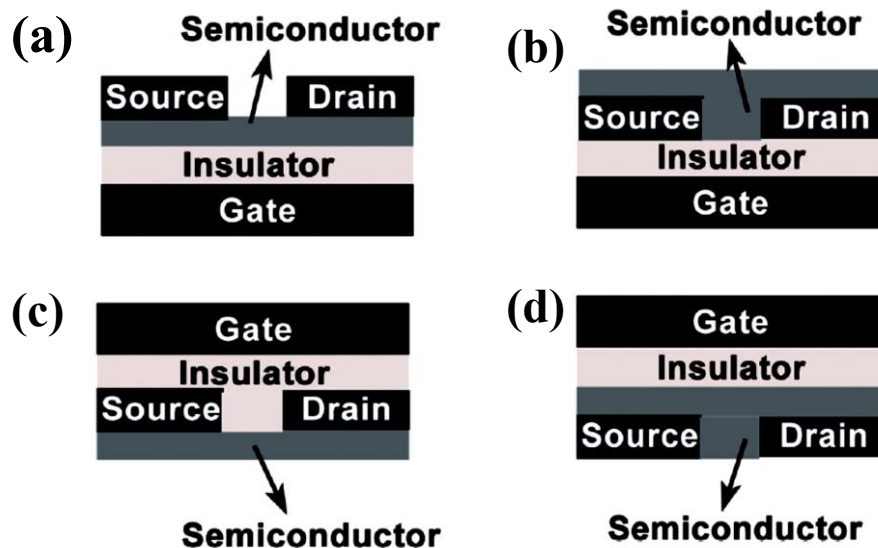
Fig. 2.17 Configurations of OTFT-based device geometries (a) bottom-gate top contact, (b) bottom gate bottom contact, (c) top gate bottom contact, (d) top gate top contact

The top contact OTFTs give better results in better charge injection, lesser contact barriers and traps, and lesser contact resistance. Any morphological chaos present at the interface of the metal-semiconductor causes contact resistance. Due to the increased surface area for charge injection, it also provided lowered charge injection resistance across the channel. Thus utilising the above properties bottom gate top contact is

fabricated in this report. In contrast to MOSFETs, OTFTs required the accumulation of injected charge carriers whereas inversion occurs in MOSFETs In general, FETs (MOSFETs) are employed when the insulator is oxide. The fundamental operation of a FET is the current fluctuation between the source and drain electrodes brought on by the imposed bias at the gate electrode. Only p-type conjugated polymers will be discussed to understand the process at the semiconductor-insulator interface when various biases are given to the metal with respect to the ground. There are three possible cases with respect to the potential applied to the gate electrode: First, when the gate electrode bias (V_{GS}) equals the flat band bias (V_{FB}). This is known as the flat band situation, in which the Fermi levels of the semiconductor and gate electrode are aligned. Second, when a negative bias is supplied to the gate electrode, the Fermi energy level is elevated. As a result, the semiconductor bands bend upwards, and positive charges accumulate in the valence band at the interface to compensate for the negative charges on the gate. This is the accumulation regime, in which charges build up at the semiconductor-insulator interface and create a hole current channel between the source and drain electrodes. This is referred to as the *on-current* state. The Fermi level of the gate electrode will decrease when a positive bias (greater positive of VFB, Figure 4c) is applied. The bands of the semiconductor will bend downward in this example, which is the opposite of the previous one. This will result in a minor buildup of negative charges in the conduction band and a slight depletion of positive charges in the valence band. The depletion state or regime is what is meant by this. The current flow between the source- and drain electrodes will be very low in this regime due to the extremely low charge density, often many orders of magnitude lower than the on-current. OTFTs, do not experience an inversion regime, in contrast to inorganic semiconductors. There are two primary causes:(i)Minority carrier injection is halted due to a high injection barrier at the source electrode, and (ii) The organic semiconductor's minority carriers are there, but they are trapped in the material, making them immobile. As a result, *off-current* is mostly caused by the majority of carriers and mainly because of doping or leakage. Up to 1-3 nm from the semiconductor-dielectric contact, the majority of charge carriers are present.
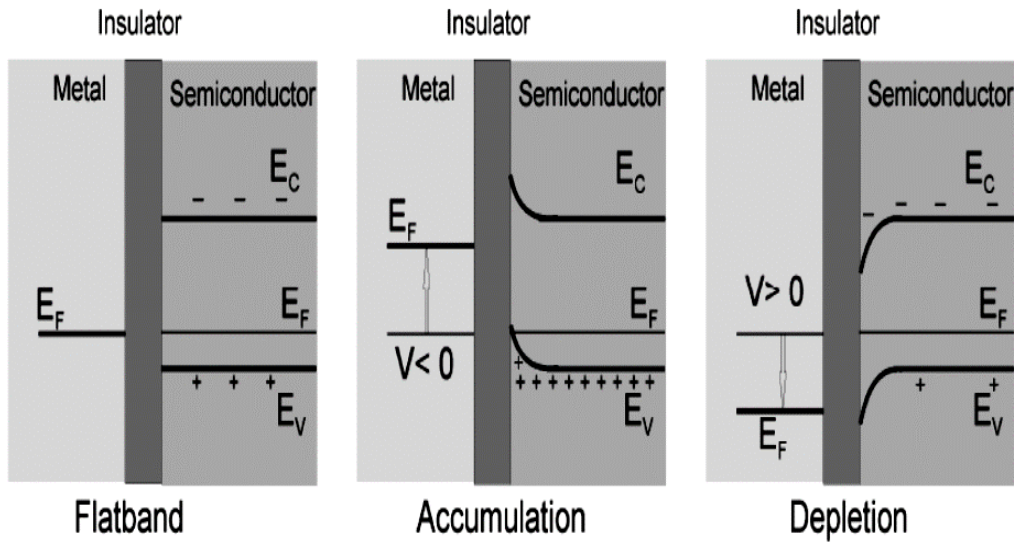
Fig. 2.18 The illustration depicts three scenarios for a p-type semiconductor in an OFET: (a) The flat-band condition when no bias is applied. (b) Accumulation regime when the metal is subjected to a negative bias (c) Depletion regime in which the metal is biassed positively [264].

In OTFTs, charge conduction is achieved with the help of injected charge carriers by applied bias. When a negative bias is placed at the gate electrode for a p-type semiconductor, holes are injected from the source electrode. The voltage applied between the source and drain electrodes is known as source-drain voltage (V_D). Gate voltage(V_G). affects how much current flows across the semiconductor layer. Charges are introduced into the semiconductor layer on the other side of the gate electrode, which together constitute the capacitor. The applied bias at the drain electrode then makes the charge mobile. The device is "off" when no voltage is supplied to the gate electrode, which prevents charge transfer. The gadget "turns on" when the gate voltage is applied, starting the transit of mobile charge carriers. Fig. 2.18 depicts the effect of a

gate electrode inducing charge, also known as the field effect. The location of the semiconductor film's HOMO and LUMO in relation to the source and drain electrodes' Fermi levels is depicted in Fig. 2.18(a). The gate bias is zero in this instance. There are no mobile charges in the semiconductor, therefore even with a tiny source-drain bias, there would be no conduction. The situations when a positive gate voltage is provided with $V_D = 0$ and $V_D > 0$, respectively, are shown in parts (b) and (d) of Fig. 2.19. At the organic/insulator interface, the application of a positive gate voltage results in a significant electric field. Due to the fixed Fermi levels of the metal contacts' externally regulated potentials, this field causes the HOMO and LUMO levels in the semiconductor to drop down (below in energy It is possible for electrons to go from the contacts into the LUMO if the gate field is big enough for the LUMO to resonate with the Fermi levels of the contacts (Fig. 2.19(b)). Now, mobile electrons at the semiconductor/insulator interface cause an electric current to flow between the source and drain when a drain voltage is applied (see Fig. 2.19(d)). The same logic holds true for negative gate bias (Fig. 2.19(c,e)). Positively charged holes are left behind when electrons leak out of the semiconductor and into the contacts due to a shift in the HOMO and LUMO levels, which causes the HOMO to resonate with the contact Fermi levels. Now, Fig. 2.19(e) shows that these holes are the mobile charges that move in response to an applied drain voltage. Regardless of the gate voltage's sign, the source electrode is always the contact that injects charges in Fig. 2.19(d,e).
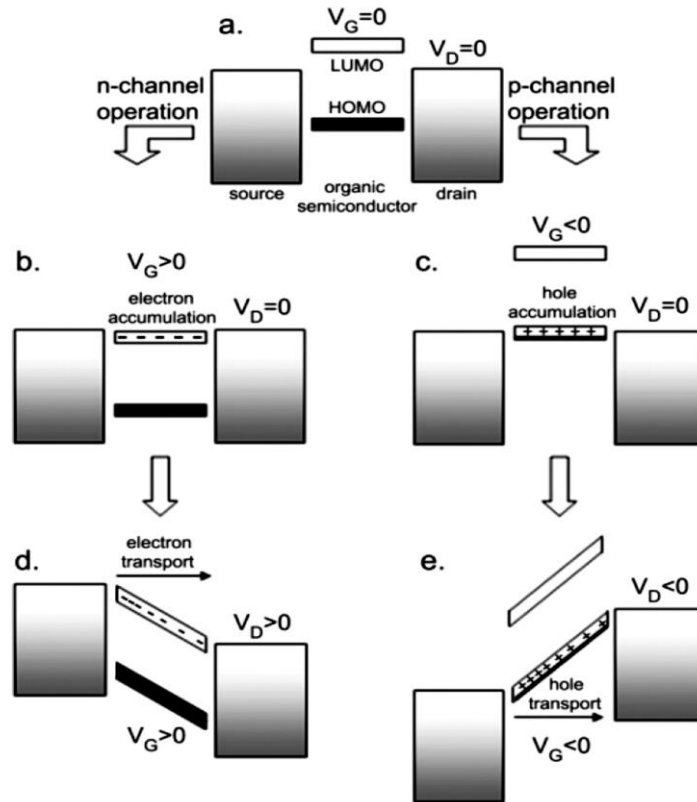
Fig.2.19 (a)An organic TFT's energy level diagram at V$_G$=0 and V$_D$=0. (b-e) show the field effect transistor operation principle for (b) electron accumulation and (d) transport and(c) hole accumulation and (e) transport [265]

2.2.17. Current-Voltage characteristics parameters extraction in OTFT

The equations to illustrate the transport characteristics in MOSFET devices are also applicable to OTFT devices:

$$I_{DS} = \frac{W}{L}\mu C_{ox}\left\{\left(V_{GS} - 2\phi_b - \frac{V_{DS}}{2}\right)V_{DS} - \frac{2}{3}\frac{\sqrt{2\varepsilon_s q N_a}}{C_i}\left[\left(V_{DS} + 2\phi_b\right)^{3/2} - \left(2\phi_b\right)^{3/2}\right]\right\} \tag{2.6}$$

Where W and L denote the width and length of the channel, respectively.μ is known as the field effect mobility in cm^2/Vs., C_{ox} represents the oxide capacitance per unit area

(F/cm2), ε_s represent the permittivity of the semiconductor (F/m), The potential difference between the Fermi level and the intrinsic Fermi level is represented by ϕ_b (V), N_a represents the doping level of the p-type substrate, and q represents the elementary charge of an electron (C). This equation **(2.6)** shows the relationship between V_{DS} and I_{DS} shows the drain current increases linearly with respect to V_{DS} and is the linear region of operation and saturation is achieved when V_{DS} is equal to the V_{GS}. The OTFT-based devices are operated in a saturation regime whereas the MOSFET devices are operated in the inversion regime. The equation **(2.6)** is simplified for the OTFT devices as:

$$I_{DS} = \frac{W}{L} \mu C_{ox} \left(V_{GS} - V_{th} - \frac{V_{DS}}{2} \right) V_{DS} \qquad (2.7)$$

Where,

$$V_{th} = \frac{qNt}{C_i} \qquad (2.8)$$

Here, N depicts the density of dopant centres and t is channel thickness. The equation **(2.7)** is based on two major assumptions: first, that the channel length is much greater than the dielectric thickness, and second, that mobility is constant. The OTFT devices operate in a linear regime when $V_{DS} << V_{GS}-V_{th}$ and in the saturation regime when $V_{DS} \geq V_{GS}-V_{th}$.

$$I_{DS}^{Lin.} = \frac{\mu C_i W}{2L} (V_{GS} - V_{th} - \frac{V_{DS}}{2}) V_{DS}; \qquad |V_{DS}| << |V_{GS} - V_{th}| \qquad (2.9)$$

$$I_{DS}^{Sat.} = \frac{\mu C_i W}{2L} (V_{GS} - V_{th})^2; \qquad |V_{DS}| \geq |V_{GS} - V_{th}| \qquad (2.10)$$

In the linear regime, equation **(2.9)** is used, for the mobility μ and threshold voltage V_{th} values. These values are extracted by plotting the I_{DS} vs V_{GS} curve. The curves are linear and follow the ohms law, where drain current is directly proportional to gate and drain voltages. In the saturation regime, equation **(2.10)** is used to determine the mobility μ and threshold voltage V_{th} values by taking the square root of the equation and getting the equation of the line

$$\sqrt{I_{DS}^{Sat.}} = \sqrt{\frac{W}{2L}C_i\mu}\left(V_{GS} - V_{th}\right) = PV_{GS} - Q \qquad (2.11)$$

From the linear fit equation of **(2.11)**, V_{th} and μ are extracted graphically. P and Q are slope and intercept at the y-axis respectively.

$$\mu = \frac{2L}{WC_i}P^2 \qquad (2.12)$$

$$V_{th} = -\frac{Q}{P} \qquad (2.13)$$

Thus the mobility and threshold values are extracted using Eqn. (**2.12**) and (**2.13**). In all OTFT-based devices, this saturation regime of operation is generally used. The Transfer characteristics (I_{DS} vs V_{GS}) are plotted on a semi-logarithmic scale. The on/off ratio is calculated by dividing the current when saturated when the device is turned on by the current when the device is turned off, i.e. before turning on the voltage.